



1 **A comparison of pre-Millennium eruption (946 AD) and modern temperatures**  
2 **from tree rings in the Changbai Mountain, northeast Asia**

3

4 **Running Title: Millennial changes in temperature of Changbai Mt.**

5

6 Haibo Du<sup>1</sup>, Michael C. Stambaugh<sup>2</sup>, J. Julio Camarero<sup>3</sup>, Mai-He Li<sup>1,4</sup>, Dapao Yu<sup>5</sup>,  
7 Shengwei Zong<sup>1</sup>, Hong S. He<sup>2\*</sup>, Zhengfang Wu<sup>1\*</sup>

8 <sup>1</sup> Key Laboratory of Geographical Processes and Ecological Security in Changbai  
9 Mountains, Ministry of Education, School of Geographical Sciences, Northeast  
10 Normal University, Changchun 130024, China

11 <sup>2</sup> School of Natural Resources, University of Missouri, Columbia, Missouri, USA

12 <sup>3</sup> Instituto Pirenaico de Ecología, IPE-CSIC, 50059 Zaragoza, Spain

13 <sup>4</sup> Swiss Federal Institute for Forest, Snow and Landscape Research WSL, 8903  
14 Birmensdorf, Switzerland

15 <sup>5</sup> CAS Key Laboratory of Forest Ecology and Management, Institute of Applied  
16 Ecology, Chinese Academy of Sciences, Shenyang, 110016, China

17

18 **Correspondence to:** wuzf@nenu.edu.cn; HeH@missouri.edu



19 **Abstract:** High-resolution temperature reconstructions in the prior millennium are  
20 limited in northeast Asia, but important for assessing regional climate dynamics. Here,  
21 we present, for the first time, a reconstruction of April temperature for ~300 years  
22 before the Millennium volcanic eruption in 946 AD, using tree rings of carbonized  
23 logs buried in the tephra in Changbai Mountain, northeast Asia. The reconstructed  
24 temperature changes were consistent with previous reconstructions in China and  
25 Northern Hemisphere. The influences of large-scale oscillations (e.g., El  
26 Niño-Southern Oscillation) on temperature variability were not significantly different  
27 between the period preceding the eruption and that of the last ~170 years. However,  
28 compared to the paleotemperature of the prior millennium, the temperature changes  
29 were more complex with stronger temperature fluctuations, more frequent  
30 temperature abruptions, and a weaker periodicity of temperature variance during the  
31 last one and half centuries. These recent changes correspond to long-term  
32 anthropogenic influences on regional climate.

33

34 **Keywords:** Carbonized logs; Changbai Mountain; dendroclimatology; Millennium  
35 volcanic eruption; temperature reconstruction; tree rings.



36 **1. Introduction**

37 The observed global mean surface temperature for the decade 2011-2020 was  
38 ~1.09 °C higher than the average over the 1850-1900 period, reflecting the warming  
39 trend since pre-industrial times (IPCC, 2021). Century-wide predictions have been  
40 made based on relatively short-term observations, which bear great uncertainties  
41 especially at local and regional spatial scales. Different from the short instrumental  
42 records, reconstructing long-term climate variability using annually-resolved proxies  
43 such as tree rings is important for analyzing the long-term variations in climate and  
44 discriminating among natural and anthropogenic factors that drive climate change  
45 (Wang et al., 2018). Long-term, historical dendroclimatic reconstructions of  
46 temperature are essential to validate global climate models and provide important  
47 inputs to understand vegetation succession and vegetation-climate relationships in the  
48 region (Schneider et al., 2015).

49

50 Tree rings are excellent proxies for high-resolution climate reconstruction. Several  
51 millennial-scale annual climate reconstructions have been developed by multiproxy  
52 data for the globe (Consortium et al., 2013; Mann et al., 2008; Mann and Jones, 2003),  
53 North Hemisphere (Guillet et al., 2017; Moberg et al., 2005; Mann et al., 1999) or  
54 North Hemisphere extratropical regions (Schneider et al., 2015; Ljungqvist, 2010).  
55 Some millennial temperature reconstructions with very coarse temporal resolution  
56 using other proxies were also completed in northeast Asia, e.g., using varved sediment



57 in Lake Sihailongwan (Chu et al., 2011). However, the millennial-scale and  
58 high-resolution climate reconstructions rarely include tree-ring proxies from northeast  
59 Asia due to limited available tree records prior to the last millennium.

60

61 The Changbai Mountain is the highest mountain in northeast Asia and encompasses  
62 all life zones found along altitudinal gradients from temperate forests to the alpine  
63 tundra (Zhou et al., 2005). Tree radial growth is sensitive to climate change in the  
64 Changbai Mt which has allowed building several dendroclimatic reconstructions for  
65 the past centuries (Lyu et al., 2016; Zhu et al., 2009; Shao and Wu, 1997). The highest  
66 peak of Changbai Mt. with origins from an intraplate stratovolcano (Tianchi volcano)  
67 located on the border between China and North Korea (Sun et al., 2014). A Plinian  
68 eruption occurred around 1000 AD (well-known as the ‘Millennium Eruption’) with a  
69 volcanic explosivity index of 7 based on an estimated eruptive column of ~25-35 km  
70 and a total tephra volume of ~100 km<sup>3</sup> (Wei et al., 2003; Horn and Schmincke, 2000).  
71 The eruption destroyed most plants within a ~50-km-radial area, but many trees  
72 buried by volcanic ash became carbonized logs (Cui et al., 1997). These carbonized  
73 logs provide a unique material to reconstruct climate of Changbai Mt. prior to the  
74 millennium eruption using tree-ring records as climate proxies.

75

76 Numerous studies have attempted dating of the Millennium Eruption (Chen et al.,  
77 2016; Xu et al., 2013; Yin et al., 2012). Recently, this eruption has been dated to the



78 end of 946 AD using a conspicuous dating marker of the ephemeral burst of  
79 cosmogenic radiation in 775 AD (Oppenheimer et al., 2017; Büntgen et al., 2014) and  
80 historical documents (Yun, 2013). With this date, carbonized trees provide the  
81 opportunity to reconstruct climate before 946 AD in Changbai Mt., a region where the  
82 greatest increase in air temperature over China was recorded during the last century  
83 (Ding et al., 2007).

84

85 Here, we analyze tree rings from the carbonized logs and modern trees on Changbai  
86 Mt. to reconstruct and compare temperatures between the three centuries  
87 pre-Millennium Eruption and the last two centuries (1885-2012). These temperature  
88 reconstructions can reveal the long-term regional climate dynamics in northeastern  
89 China or even Northeast Asia and allow characterizing recent features related to  
90 anthropogenic climate warming.

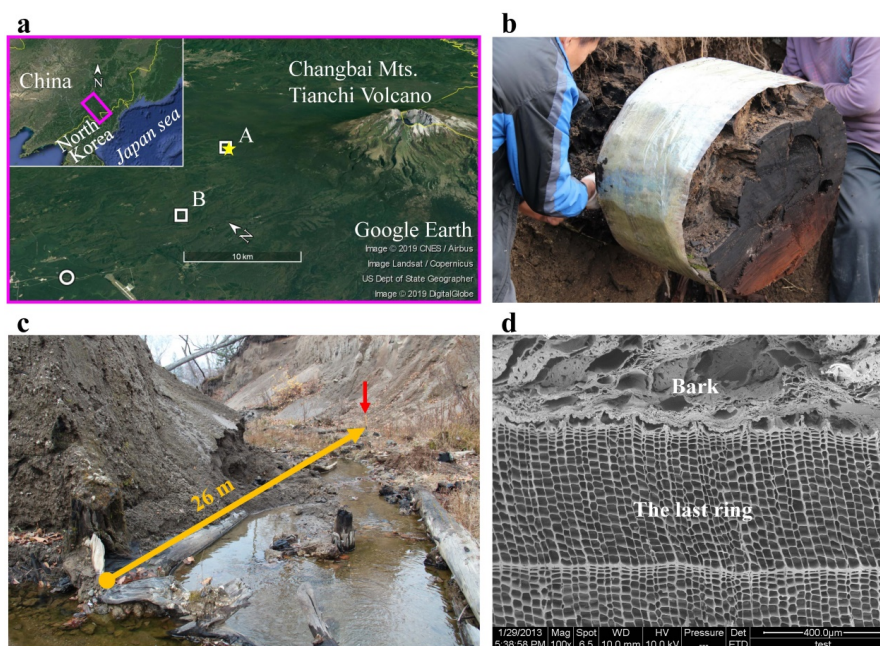
91

## 92 **2. Material and methods**

93 The Changbai Mt. ranges from 713 to 2691 m a.s.l., and belongs to the temperate  
94 continental and mountain climate, with an annual mean temperature ranging from -7.3  
95 to 4.9 °C and annual precipitation from 800 to 1800 mm (Du et al., 2018). The period  
96 of cambial growth of trees is approximately May to September at low altitudes (e.g.,  
97 1000 m a.s.l.) and shortens to June to August at high altitudes (e.g., treeline located at  
98 ~2060 m a.s.l.) (Du et al., 2021).



99 We sampled 55 carbonized trees from two nearby sites on the western slope of  
100 Changbai Mt. in 2012 and 2013 (site A, 42°9' N, 127°52' E, 1025 m a.s.l., with 33  
101 samples; and site B, 42°5.7' N, 127°42.4' E, 892 m a.s.l., with 22 samples) (Figure 1a,  
102 b, c). Most of these trees had bark indicating the last year of tree growth was present  
103 (Figure 1d). Radiocarbon dating of the wood of the outermost rings of two trees (from  
104 sites A and B, respectively; Figure 1a) was conducted in the Accelerator Mass  
105 Spectrometry (AMS) Laboratory at Peking University (Table 1) and indicated that  
106 these trees died during the Millennium Eruption in 946 AD. Other carbonized trees  
107 found and reported in previous studies were also dead in 946 AD (e.g., Oppenheimer  
108 et al., 2017; Xu et al., 2013; Yin et al., 2012). Many of these carbonized tree samples  
109 were not totally carbonized (Figure 1b) and showed a complete tree trunk (Figure 1c),  
110 indicating that little or no transport has occurred from their original location.



111



112 **Figure 1. (a)** Location of the Changbai Mountain and sample sites on Changbai Mt.  
113 (from Google Earth Image). White squares represent sites where the carbonized logs  
114 were found (A, Weidongzhan; B, Xiaoshahe). Yellow star shows the sampling site of  
115 the modern forest. White circle indicates the Donggang National Datum  
116 Meteorological Station. **(b and c)** Context of carbonized logs in the field. Species of  
117 logs are *Pinus koraiensis*. **(d)** Cellular characteristics of the outermost tree ring and  
118 bark of the carbonized log shown in (b).

119

120 **Table 1.** AMS  $^{14}\text{C}$  results of the complete outermost rings of two carbonized logs  
121 collected from Weidongzhan (Site A) and Xiaoshahe (Site B) on the western slope of  
122 the Changbai Mountain.

Lab ID	Site	AMS $^{14}\text{C}$ age (yr BP)*	Tree-ring calibration age (AD, $1\sigma$ (68.2%))	Tree-ring calibration age (AD, $2\sigma$ (95.4%))
BA150220	A	1155±20	780-790 AD (1.0%) 820-840 AD (7.4%) 860-900 AD (33.8%) 910-950 AD (25.9%)	770-970 AD (95.4%)
BA121692	B	1090±20	895-920 AD (24.8%) 945-990 AD (43.4%)	890-1020 AD (95.4%)

123 \* AMS  $^{14}\text{C}$  ages are dated at the Peking University AMS Laboratory and given in year  
124 BP (years before 1950).



125

126 We identified the tree species of carbonized trees by analyzing microscopic  
127 anatomical features of wood on three planes (cross-sectional, radial, and tangential)  
128 (Figure S1). Eighteen of the 55 sample trees were Korean pine (*Pinus koraiensis*  
129 Siebold & Zucc.). We used these trees to reconstruct the climate before the  
130 Millennium Eruption (946 AD) using the current climate response of Korean pine  
131 growth (Zhu et al., 2009). Prior to performing the climate response analyses, we also  
132 sampled modern living Korean pines. Core samples from 27 living Korean pine trees  
133 located near site A (see Figure 1a) were collected in 2013 and at 1.3 m height using a  
134 Pressler increment borer.

135

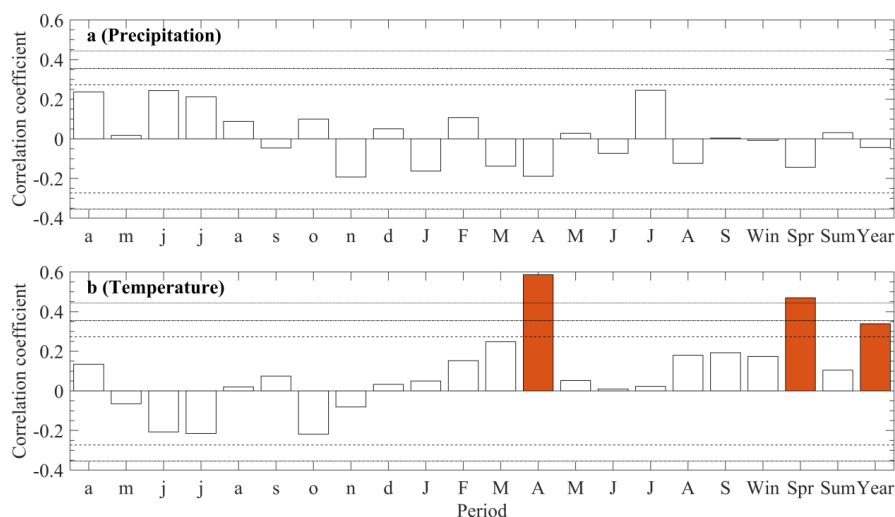
136 Tree-ring width measurements and chronology development of carbonized and living  
137 samples were conducted using standard dendrochronological techniques (Cook and  
138 Kairiukstis, 2013). All available wood cross-sections/cores were first visually  
139 cross-dated after cutting or sanding the wood surface, and then the quality of the  
140 cross-dating was checked using the COFECHA program (Holmes, 1983). Age  
141 detrending of the ring-width series was performed by fitting negative exponential  
142 curves and calculating ring-width indices through the ratio method (Fritts, 1976).  
143 Then, autoregressive modeling was used to remove first-order autocorrelation and to  
144 obtain pre-whitened or residual series of ring-width indices. Standardized (STD) and  
145 residual (RES) growth chronologies, with or without first-order autocorrelation



146 respectively, were developed by calculating robust biweight means using the  
147 ARSTAN program version 49 (Cook et al., 2017; Cook, 1985). Then, subsample  
148 signal strength (SSS) was used to evaluate the suitability and reliability of chronology  
149 data for climate reconstructions (Buras, 2017; Wigley et al., 1984). The  $SSS > 0.85$   
150 was used to determine the robust and maximum chronology length and to ensure the  
151 reliability of the reconstructions (Figure S2). This threshold corresponded to a  
152 minimum sample depth of 12 samples for the carbonized tree chronology (from 746  
153 AD) and 14 samples for the living tree chronology (from 1885 AD onwards).

154

155 Instrumental climate data were obtained for the period 1961-2012 from the Donggang  
156 National Datum Meteorological Station (42°6' N, 127°34.2' E, 851 m a.s.l., situated  
157 15-22 km apart from the sample sites; source: China Meteorological Data Network,  
158 <http://data.cma.gov.cn/>). We calculated the Pearson correlation coefficients between  
159 both chronologies and different time-scale (monthly, seasonal and annual) climate  
160 variables (precipitation, mean temperature) to identify the main climate factors  
161 driving tree growth. Correlations were calculated from prior April to current  
162 September. Besides, to remove the trend effects, the correlation coefficients between  
163 the first-order difference series of chronology and climate variables were also  
164 calculated to further explore their relationships. Because the RES chronology (Figure  
165 2) showed to be more highly correlated with climate than the STD chronology  
166 (Figures S3-S5), we used the RES chronology to reconstruct temperature.



167

168 **Figure 2.** Pearson correlation coefficients between the RES tree-ring chronology and  
169 monthly, seasonal and annual (a) precipitation and (b) temperature during 1961-2012.  
170 Lowercase and uppercase letter on x axis indicate the months of the previous and  
171 current year, respectively. The horizontal dotted, dash-dotted, and dashed lines  
172 represent significance levels of 0.001, 0.01, and 0.05, respectively. Bars with  
173 significant correlation are filled with red colour.

174

175 We used a linear regression model to reconstruct past climate from the RES tree-ring  
176 chronology. The reliability of the regression model was evaluated using split sample  
177 calibration-validation statistics whereby calibration was conducted for 1961-1986 and  
178 validation was done for 1987-2012, after which the periods were switched and the  
179 process repeated (Table 2). Model statistics included the Pearson correlation  
180 coefficient, coefficient of determination ( $R^2$ ), reduction of error (RE), coefficient of  
181 efficiency (CE), Durbin-Watson test (DW), root-mean-square error (RMSE), and



182 mean absolute error (MAE). Any positive RE/CE is generally accepted as indicative  
183 of reasonable skill in the reconstructions (Cook et al., 1994; Briffa et al., 1988; Fritts,  
184 1976). The DW statistic tests the temporal autocorrelation in the residuals between  
185 modelled and observed climate data.

186

187 **Table 2.** Calibration/verification statistics of the temperature reconstruction.

	Calibration	Verification	Calibration	Verification	Calibration
	1961-1986	1987-2012	1987-2012	1961-1986	1961-2012
Years	26	26	26	26	52
Correlation	0.51	0.66	0.66	0.51	0.59
$R^2$	0.26	0.43	0.43	0.26	0.34
RE	--	0.40	--	0.24	--
CE	--	0.35	--	0.17	--
DW	2.28	2.16	2.16	2.28	2.16
RMSE	1.43	1.44	1.35	1.52	1.41
MAE	1.13	1.13	1.01	1.19	1.10

188 Correlation,  $R^2$ , and DW were calculated between instrumental April temperature and  
189 RES tree-ring width chronology. Reduction of error (RE), coefficient of efficiency  
190 (CE), root-mean-square error (RMSE) and mean absolute error (MAE) were  
191 calculated between instrumental and reconstructed April temperatures.

192



193 To analyze the abrupt changes in temperature between both periods, we calculated the  
194 changes in mean state of temperature reconstructions using a heuristic segmentation  
195 algorithm (the imposed minimum length of segments is 35 years) developed by  
196 Bernaola-Galván et al. (2001). This method has been widely used to determine the  
197 abrupt changes in mean state of a chronology (Gong et al., 2006). The significance of  
198 the changes was estimated by the  $t$  test.

199

200 Power spectrum analysis was applied to investigate the reasonable periodicities in our  
201 climate reconstructions. We used the wavelet analysis with a Morlet wavelet to  
202 examine the periodicity of the reconstructed series and to check how periodicity  
203 changes through time (Torrence and Compo, 1998). This analysis was separately  
204 performed over the two ranges of the reconstructions. These analyses were carried out  
205 using the Matlab R2019b software.

206

### 207 **3. Results and Discussion**

#### 208 3.1. Temperature reconstruction

209 Precipitation in all months and seasons showed no significant correlation with the  
210 RES chronology (Figure 2a). This was expected since the study area is wet, and  
211 moisture-deficits that limit plant growth are uncommon. However, mean temperature  
212 in April showed a positive and significant ( $p < 0.001$ ) correlation ( $r = 0.59$ ) with the  
213 RES chronology during 1961-2012 (Figure 2b), indicating that the radial growth of



214 Korean pine is primarily limited by temperature in the month preceding cambial onset.  
215 Moreover, the correlation coefficients for the first-order difference series indicated  
216 that chronologies still have statistically significant and strongest relationship with  
217 April temperature (Figures S4-S5). These are similar to the findings for Korean pine  
218 growth found in north of Changbai Mt. (Zhu et al., 2009) and more broadly across  
219 northeast Asia (Wang et al., 2017). Other species in other cold regions show  
220 consistent growth responses to pre-growth temperature as a limiting factor in annual  
221 radial growth (e.g., Hinoki cypress (*Chamaecyparis obtuse*) in central Japan  
222 (Yonenobu and Eckstein, 2006), Georgei fir (*Abies georgei*) in the southeast Tibetan  
223 Plateau (Liang et al., 2009), and Scots pine (*Pinus sylvestris L.*) in northern Poland  
224 (Koprowski et al., 2012)). A positive growth response to April temperature can occur  
225 due to warming in the period prior to the growing season causing tree dormancy to  
226 break early, accelerating the division and enlargement of cambial cells, and extending  
227 the length of the growing season (Schweingruber, 1996). The correlation between the  
228 RES chronology and spring temperature is also significant, mainly due to the effects  
229 of April temperature.

230

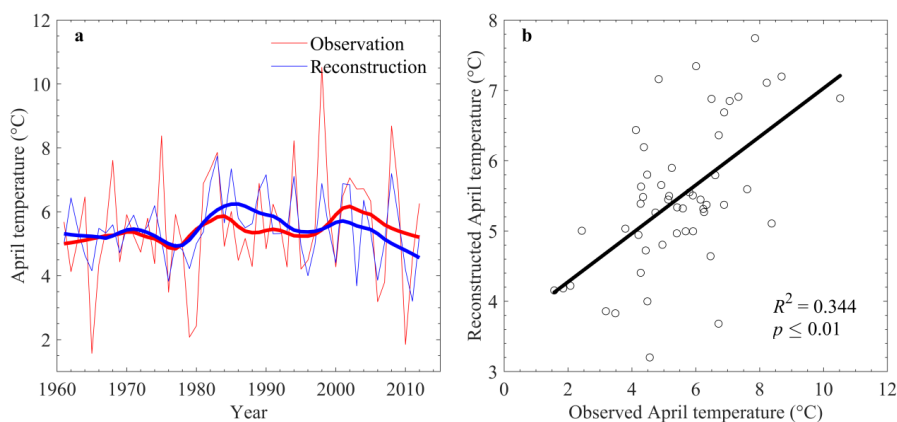
231 The positive RE (0.40) and CE (0.35) statistics for the late verification period and  
232 positive RE (0.24) and CE (0.17) statistics for the early verification period indicated  
233 reasonable reconstruction skill for both compared sub-periods (Table 2). Therefore,  
234 we used the full calibration period for developing April temperature model by



235 calculating the model  $R^2$ , DW (Durbin-Watson statistic), RMSE, and MAE (Table 2).  
236 The DW statistic calculated over the full calibration period ( $DW_{1961-2012} = 2.16$ ,  $p <$   
237  $0.01$ ), achieving a value close to the optimal value of 2 which indicates no significant  
238 autocorrelation in the residuals. The full tree-ring model predicting April temperature  
239 was given as:

$$240 \quad y = 7.38 * RES - 1.79 \quad (1);$$

241 where  $y$  is April temperature and  $RES$  is the residual tree-ring index, being the model  
242 and the predictor variables significant at  $p < 0.01$ . This regression model accounted  
243 for 34% of the variance in instrumental April temperature (Figure 3b). The  
244 reconstructed April mean temperature showed decreasing trend after 2000, which was  
245 different from the results of reconstructed April-July minimum temperature by Lyu et  
246 al. (2016) and February-April temperature by Zhu et al. (2009). However, the  
247 decreasing trend was coincident with the change in the observed April temperature  
248 (Figure 3a). Therefore, the difference of the change in temperature during the last  
249 decade between the temperature reconstructions may be due to seasonal diversity or  
250 regional difference. Besides, although the reconstruction underestimates the extreme  
251 temperatures recorded in some years (e.g., 1965 and 1998), it successfully captures  
252 both high and low frequency variations of temperature variability (Figure 3a).



253

254 **Figure 3.** (a) Observed (red thin line) and reconstructed (blue thin line) annual April  
255 temperature. Heavy lines are the corresponding 13-year moving averaged  
256 temperatures. (b) Linear regression between observed and reconstructed temperatures  
257 during the period 1961-2012.

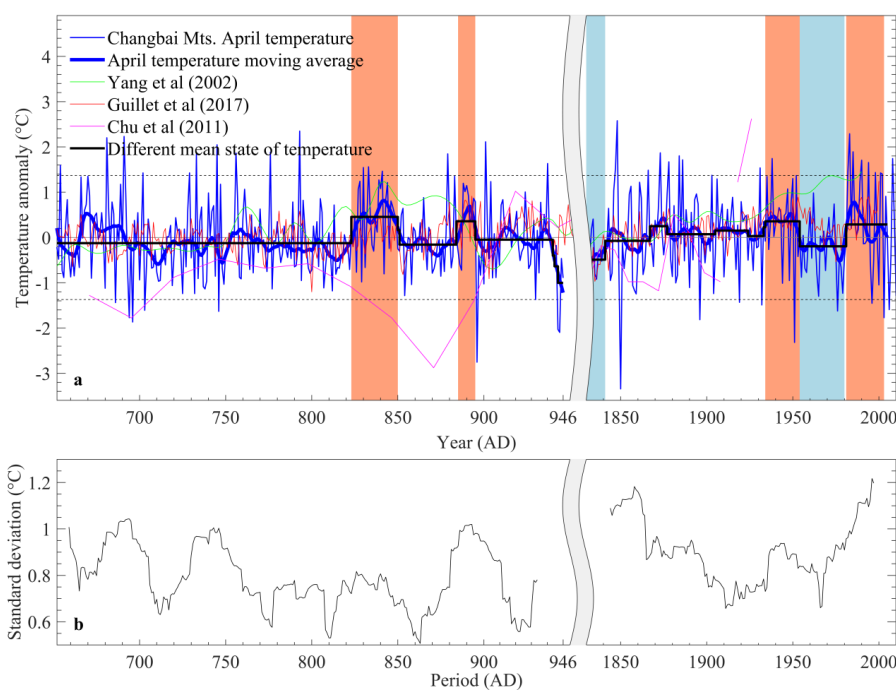
258

### 259 3.2. Comparisons between changes in paleoclimate and modern climate

260 Based on the regression model, we reconstructed the annual April temperature and a  
261 13-year moving average for periods 652-946 AD and 1830-2012 AD (Figure 4a).  
262 Truncated periods of reconstructions where SSS is  $> 0.85$  were 746-946 AD and  
263 1885-2012 AD. Although our temperature reconstructions did not match well with the  
264 previous temperature reconstructions using the varved sediment in Lake Sihailongwan  
265 in the Changbai Mt. (Chu et al., 2011), both temperature reconstructions showed  
266 coincident decreasing-increasing-decreasing variation during 850-946 AD. The lack  
267 of agreement between these two proxies may be due to age model error inherent in  
268 radiocarbon-dated records (Conroy et al., 2010). For regional scale, our temperature



269 reconstructions generally coincided with the variations of pre-millennial temperature  
270 in China (Yang et al., 2002). Interestingly, variations in April temperature  
271 reconstructions in both two periods in this study are similar to those observed in  
272 summer temperature reconstructions for Northern Hemisphere (Guillet et al., 2017).  
273 These temperature reconstructions all display warm periods in 830-850 AD, 885-895  
274 AD, 1931-1953 AD, 1981-2000s AD, and cold periods in 1830-1840 AD and  
275 1955-1980 AD.



276  
277 **Figure 4.** (a) Reconstruction of April temperature anomaly (blue thin lines) for  
278 652-946 AD and 1830-2012 AD, with a 13-year moving average (blue bold lines) for  
279 Changbai Mt. The temperature anomaly is relative to the mean during the entire  
280 period. Green, red, and magenta lines indicate standardized temperature anomalies in



281 China (“H-res”) (Yang et al., 2002), the summer temperature anomalies for Northern  
282 Hemisphere (Guillet et al., 2017) and temperature anomalies using the varved  
283 sediment in Lake Sihailongwan in the Changbai Mt. (Chu et al., 2011), respectively.  
284 Black bold lines show the changes in mean state of the April temperature  
285 reconstructions. **(b)** Time series of standard deviation of 30-year moving window for  
286 the April temperature reconstructions in this study. A given period (e.g., 900 AD)  
287 represents a standard deviation in 30 years before and after that period (e.g., 886-915  
288 AD).

289

290 During 746-946 AD, the standard deviation (s.d.) of reconstructed mean April  
291 temperature was 0.77 °C, whereas the standard deviation was 0.92 °C for the period  
292 1890-2012. That is, temperature variance (standard deviation) increased 18% for  
293 modern temperature in comparison to the temperature prior to the 946 AD Millennium  
294 Eruption. Moreover, the 30-year moving standard deviations showed periodical  
295 change and smaller values during the pre-eruption period than those in the last 180  
296 years (Figure 4b). Specifically, the 30-year moving temperature variance showed  
297 significant ( $p < 0.05$ ) periodicity of 50-70 years (Figure S6ab). However, there was no  
298 significant periodicity of temperature variance during the last 180 years (Figure  
299 S6cd).

300

301 There were only five periods with significant differences in mean state of temperature



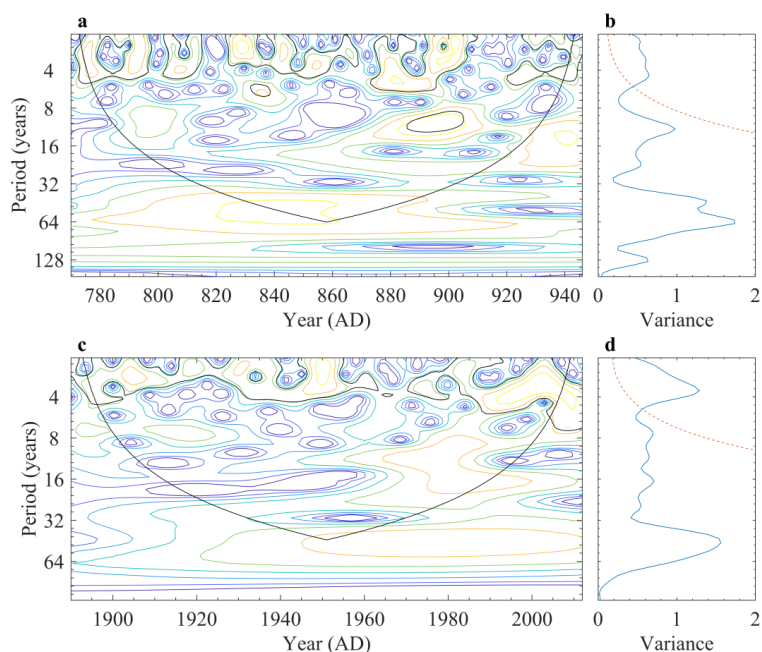
302 during the last 200 years before the volcano eruption (Figure 4a). The two warm  
303 periods in 830-850 AD and 885-895 AD were widely recognized as warm epochs also  
304 by other temperature reconstructions for Northern Hemisphere extratropical areas  
305 (e.g., Esper et al., 2002). In contrast, nine periods with significantly different mean  
306 temperature states were revealed during the last ~180 years before present. Moreover,  
307 only nine warm years (defined as  $> 1.5$  s.d.; years: 756, 776, 793, 830, 833, 841, 879,  
308 901, 937) and 5 cold years (defined as  $< 1.5$  s.d.; years: 746, 896, 930, 943, 944) were  
309 identified during the last 200 years before the Millennium Eruption, whereas 19 warm  
310 years (1847, 1848, 1866, 1873, 1878, 1884, 1886, 1903, 1931, 1938, 1982, 1983,  
311 1985, 1990, 1994, 1998, 2001, 2002, 2008) and 10 cold years (1850, 1896, 1919,  
312 1932, 1951, 1976, 1996, 2003, 2006, 2011) were identified during the last 170 years  
313 before present (Figure 4a).

314

315 These differences may be partly due to the anthropogenic influences since  
316 approximately the beginning of the Industrial Revolution (Gong et al., 2006). For  
317 example, the probability of present-day hot extremes increased 1-1.2% relative to  
318 pre-Industrial Revolution time in the region of Changbai Mt. Presently, 75% of the  
319 moderate hot extremes occurring worldwide are attributable to climate warming, of  
320 which the majority are extremely likely to be anthropogenic (Fischer and Knutti,  
321 2015). Higher 30-year standard deviations during the last 180 years than the  
322 pre-eruption period may also support the attribution to increased anthropogenic



323 influences on thermal conditions (Figure 4b).  
324  
325 Wavelet analysis indicated significant ( $p < 0.05$ ) periodicity of  $\sim 4.5$  years during  
326 770-946 AD (Figure 5ab) and  $\sim 3.6$  years during the last  $\sim 120$  years (Figure 5cd).  
327 Similar periodicities of 3 to 4 years were also found in previous analyses of  
328 instrumental and reconstructed temperatures (Zhang et al., 2013; Yu et al., 2013; Chen  
329 et al., 2010). Although our temperature reconstructions do not contain the significant  
330 ( $p < 0.05$ ) quasi-11-year periodicity (e.g., Li et al., 2011) during the entire period, the  
331 significant ( $p < 0.05$ ) quasi-11-year periodicity in 880-910 AD and the non-significant  
332 quasi-11-year period in 785-810 AD and 850-870 AD were found. Significantly short  
333 periodicities are typically associated with El Niño-Southern Oscillation (ENSO)  
334 (Stone et al., 1998; Allan et al., 1996) and temperature in March to May in northeast  
335 China is affected by ENSO (Yuan and Yang, 2012). Moreover, the changes in  
336 temperature in northeast China correspond to the quasi-4-year changes in sea surface  
337 temperature in the central and eastern Pacific Ocean, suggesting a close link between  
338 temperature variation in northeast China and the ENSO cycle (Zhu et al., 2004).  
339 These results indicate that the effects of some large-scale oscillations (e.g., ENSO) on  
340 paleo- and modern- temperature continue to be important to the climate forcing in the  
341 region of Changbai Mt.



342

343 **Figure 5.** (a, c) Wavelet power spectrum of the reconstructed April temperature from  
344 (a) carbonized and (c) modern trees. The power has been scaled by the global wavelet  
345 spectrum. Black contour is the 95% confidence level using a red-noise (autoregressive  
346 lag1) background spectrum. (b, d) The global wavelet power spectrum (light blue line)  
347 for (b) carbonized trees-based and (d) modern trees-based temperature reconstruction.  
348 Dashed lines represent a significance of 0.05.

349

#### 350 4. Conclusions

351 We presented a new 295-year reconstruction of April temperature before the  
352 Millennium Eruption occurred in 946 AD at Changbai Mt. using unique tree-ring  
353 proxies of carbonized logs buried in the tephra, which was compared to that of living  
354 trees growing during the last 183 years. Temperature reconstructions correspond well



355 with previous large-regional temperature reconstructions. Our results showed that,  
356 although the influences of some internal variability (e.g., ENSO) on variation in  
357 temperature do not change between the periods, the changes in modern temperatures  
358 become more complex (e.g., increased variation and abrupt changes, and weakening  
359 in periodicity of temperature variance) than those in period prior to 946 AD likely due  
360 to anthropogenic influences. The present study provides tree-ring proxies for climate  
361 reconstructions in northeast Asia for the last millennium. Documentation of these  
362 features is important for understanding long-term regional climate dynamics and  
363 analyzing the millennial-scale changes in vegetation-climate relationship in northeast  
364 Asia.  
365



366 **Data availability**

367 Tree-ring chronology and climate data used in this study are archived at ZENODO:  
368 <https://doi.org/10.5281/zenodo.6633856>. They can also be provided by the  
369 corresponding author.

370

371 **Authors' contributions**

372 H.D., Z.W., and H.S.H. conceived and led this study. Tree rings and observation data  
373 collection was led by H.D. and S.Z. Analyses and the first draft was carried out by  
374 H.D. and M.S., and all authors contributed to revising subsequent manuscripts.

375

376 **Declaration of Competing Interest**

377 The authors declare that they have no conflict of interest.

378

379 **Acknowledgments**

380 We acknowledge support from the Joint Fund of National Natural Science Foundation  
381 of China (U19A2023) and the Fundamental Research Funds for the Central  
382 Universities (2412020FZ002).



383 **References**

- 384 Allan, R., Lindsay, J., and Parker, D.: El Niño southern oscillation & climatic  
385 variability, CSIRO Publishing, Collingwood, 405 pp, 1996.
- 386 Bernaola-Galván, P., Ivanov, P. C., Nunes Amaral, L. A., and Stanley, H. E.: Scale  
387 Invariance in the Nonstationarity of Human Heart Rate, *Phys. Rev. Lett.*, 87,  
388 168105, <https://doi.org/10.1103/PhysRevLett.87.168105>, 2001.
- 389 Briffa, K. R., Jones, P. D., Pilcher, J. R., and Hughes, M. K.: Reconstructing Summer  
390 Temperatures in Northern Fennoscandia Back to A.D. 1700 Using  
391 Tree-Ring Data From Scots Pine, *Arct. Alp. Res.*, 20, 385-394,  
392 <https://doi.org/10.1080/00040851.1988.12002691>, 1988.
- 393 Büntgen, U., Wacker, L., Nicolussi, K., Sigl, M., Gütler, D., Tegel, W., Krusic, P. J.,  
394 and Esper, J.: Extraterrestrial confirmation of tree-ring dating, *Nat. Clim.*  
395 *Change*, 4, 404, <https://doi.org/10.1038/nclimate2240>, 2014.
- 396 Buras, A.: A comment on the expressed population signal, *Dendrochronologia*, 44,  
397 130-132, <https://doi.org/10.1016/j.dendro.2017.03.005>, 2017.
- 398 Chen, S., Shi, Y., Guo, Y., and Zheng, Y.: Temporal and spatial variation of annual  
399 mean air temperature in arid and semiarid region in northwest China over a  
400 recent 46 year period, *J. Arid Land*, 2, 87-97,  
401 <https://doi.org/10.3724/SPJ.1227.2010.00087>, 2010.
- 402 Chen, X.-Y., Blockley, S. P. E., Tarasov, P. E., Xu, Y.-G., McLean, D., Tomlinson, E.  
403 L., Albert, P. G., Liu, J.-Q., Müller, S., Wagner, M., and Menzies, M. A.:



- 404 Clarifying the distal to proximal tephrochronology of the Millennium (B–Tm)  
405 eruption, Changbaishan Volcano, northeast China, *Quat. Geochronol.*, 33,  
406 61-75, <https://doi.org/10.1016/j.quageo.2016.02.003>, 2016.
- 407 Chu, G., Sun, Q., Wang, X., Liu, M., Lin, Y., Xie, M., Shang, W., and Liu, J.:  
408 Seasonal temperature variability during the past 1600 years recorded in  
409 historical documents and varved lake sediment profiles from northeastern  
410 China, *The Holocene*, 22, 785-792,  
411 <https://doi.org/10.1177/0959683611430413>, 2011.
- 412 Conroy, J. L., Overpeck, J. T., and Cole, J. E.: El Niño/Southern Oscillation and  
413 changes in the zonal gradient of tropical Pacific sea surface temperature over  
414 the last 1.2 ka, *PAGES News*, 18, 32-34, 2010.
- 415 Cook, E. R.: A time series analysis approach to tree-ring standardization, Graduate  
416 College, University of Arizona, Tucson, 1985.
- 417 Cook, E. R. and Kairiukstis, L. A.: *Methods of Dendrochronology: Applications in the*  
418 *Environmental Sciences*, Springer Netherlands, 394 pp,  
419 <https://doi.org/10.1007/978-94-015-7879-0>, 2013.
- 420 Cook, E. R., Briffa, K. R., and Jones, P. D.: Spatial regression methods in  
421 dendroclimatology: A review and comparison of two techniques, *Int. J.*  
422 *Climatol.*, 14, 379-402, <https://doi.org/10.1002/joc.3370140404>, 1994.
- 423 Cook, E. R., Krusic, P. J., Peters, K., and Holmes, R. L.: Program ARSTAN (version  
424 49), Autoregressive tree–ring standardization program. Tree–Ring Laboratory



- 425 of Lamont–Doherty Earth Observatory, USA, 2017.
- 426 Cui, Z., Zhang, S., and Tian, J.: The study on volcanic eruption and forest  
427 conflagration since holocene quaternary in Changbai Mt., *Geogr. Res.*, 16,  
428 92-97, 1997.
- 429 Ding, Y., Ren, G., Zhao, Z., Xu, Y., Luo, Y., Li, Q., and Zhang, J.: Detection, causes  
430 and projection of climate change over China: An overview of recent progress,  
431 *Adv. Atmos. Sci.*, 24, 954-971, <https://doi.org/10.1007/s00376-007-0954-4>,  
432 2007.
- 433 Du, H., Li, M.-H., Rixen, C., Zong, S., Stambaugh, M., Huang, L., He, H. S., and Wu,  
434 Z.: Sensitivity of recruitment and growth of alpine treeline birch to elevated  
435 temperature, *Agric. For. Meteorol.*, 304-305, 108403,  
436 <https://doi.org/10.1016/j.agrformet.2021.108403>, 2021.
- 437 Du, H., Liu, J., Li, M.-H., Büntgen, U., Yang, Y., Wang, L., Wu, Z., and He, H. S.:  
438 Warming-induced upward migration of the alpine treeline in the Changbai  
439 Mountains, northeast China, *Global Change Biol.*, 24, 1256-1266,  
440 <https://doi.org/10.1111/gcb.13963>, 2018.
- 441 Esper, J., Cook, E. R., and Schweingruber, F. H.: Low-Frequency Signals in Long  
442 Tree-Ring Chronologies for Reconstructing Past Temperature Variability,  
443 *Science*, 295, 2250-2253, <https://doi.org/10.1126/science.1066208>, 2002.
- 444 Fischer, E. M. and Knutti, R.: Anthropogenic contribution to global occurrence of  
445 heavy-precipitation and high-temperature extremes, *Nat. Clim. Change*, 5, 560,



- 446 <https://doi.org/10.1038/nclimate2617>, 2015.
- 447 Fritts, H. C.: Tree rings and climate, Elsevier, New York 1976.
- 448 Gong, Z.-Q., Feng, G.-L., Wan, S.-Q., and Li, J.-P.: Analysis of features of climate  
449 change of Huabei area and the global climate change based on heuristic  
450 segmentation algorithm, *Acta Phys. Sinica*, 55, 477,  
451 <https://doi.org/10.7498/aps.55.477>, 2006.
- 452 Guillet, S., Corona, C., Stoffel, M., Khodri, M., Lavigne, F., Ortega, P., Eckert, N.,  
453 Sielenou, P. D., Daux, V., Churakova, Olga V., Davi, N., Edouard, J.-L.,  
454 Zhang, Y., Luckman, Brian H., Myglan, V. S., Guiot, J., Beniston, M.,  
455 Masson-Delmotte, V., and Oppenheimer, C.: Climate response to the Samalas  
456 volcanic eruption in 1257 revealed by proxy records, *Nat. Geosci.*, 10, 123,  
457 <https://doi.org/10.1038/ngeo2875>, 2017.
- 458 Holmes, R. L.: Computer-assisted quality control in tree-ring dating and measurement,  
459 *Tree-Ring Bull.*, 43, 69-78, 1983.
- 460 Horn, S. and Schmincke, H.-U.: Volatile emission during the eruption of Baitoushan  
461 Volcano (China/North Korea) ca. 969 AD, *Bull. Volcanol.*, 61, 537-555,  
462 <https://doi.org/10.1007/s004450050004>, 2000.
- 463 IPCC: Summary for Policymakers. In: *Climate Change 2021: The Physical Science*  
464 *Basis. Contribution of Working Group I to the Sixth Assessment Report of the*  
465 *Intergovernmental Panel on Climate Change* [Masson-Delmotte, V., P. Zhai, A.  
466 Pirani, S. L. Connors, C. Péan, S. Berger, N. Caud, Y. Chen, L. Goldfarb, M. I.



- 467 Gomis, M. Huang, K. Leitzell, E. Lonnoy, J.B.R. Matthews, T. K. Maycock, T.  
468 Waterfield, O. Yelekçi, R. Yu and B. Zhou (eds.)]. Cambridge University Press.  
469 In Press, 2021.
- 470 Koprowski, M., Przybylak, R., Zielski, A., and Pospieszńska, A.: Tree rings of Scots  
471 pine (*Pinus sylvestris* L.) as a source of information about past climate in  
472 northern Poland, *Int. J. Biometeorol.*, 56, 1-10,  
473 <https://doi.org/10.1007/s00484-010-0390-5>, 2012.
- 474 Li, Z., Shi, C. M., Liu, Y., Zhang, J., Zhang, Q., and Ma, K.: Summer mean  
475 temperature variation from 1710–2005 inferred from tree-ring data of the  
476 Baimang Snow Mountains, northwestern Yunnan, China, *Clim. Res.*, 47,  
477 207-218, <https://doi.org/10.3354/cr01012>, 2011.
- 478 Liang, E. Y., Shao, X. M., and Xu, Y.: Tree-ring evidence of recent abnormal warming  
479 on the southeast Tibetan Plateau, *Theor. Appl. Climatol.*, 98, 9-18,  
480 <https://doi.org/10.1007/s00704-008-0085-6>, 2009.
- 481 Ljungqvist, F. C.: A new reconstruction of temperature variability in the extra -  
482 tropical northern hemisphere during the last two millennia, *Geogr. Ann. Ser. A*  
483 *Phys. Geogr.*, 92, 339-351, <https://doi.org/10.1111/j.1468-0459.2010.00399.x>,  
484 2010.
- 485 Lyu, S., Li, Z., Zhang, Y., and Wang, X.: A 414-year tree-ring-based April–July  
486 minimum temperature reconstruction and its implications for the extreme  
487 climate events, northeast China, *Clim. Past*, 12, 1879-1888,



- 488 <https://doi.org/10.5194/cp-12-1879-2016>, 2016.
- 489 Mann, M. E. and Jones, P. D.: Global surface temperatures over the past two millennia,  
490 *Geophys. Res. Lett.*, 30, <https://doi.org/10.1029/2003GL017814>, 2003.
- 491 Mann, M. E., Bradley, R. S., and Hughes, M. K.: Northern hemisphere temperatures  
492 during the past millennium: inferences, uncertainties, and limitations, *Geophys.*  
493 *Res. Lett.*, 26, 759-762, 1999.
- 494 Mann, M. E., Zhang, Z., Hughes, M. K., Bradley, R. S., Miller, S. K., Rutherford, S.,  
495 and Ni, F.: Proxy-based reconstructions of hemispheric and global surface  
496 temperature variations over the past two millennia, *P. Natl. Acad. Sci. USA*,  
497 105, 13252, <https://doi.org/10.1073/pnas.0805721105>, 2008.
- 498 Moberg, A., Sonechkin, D. M., Holmgren, K., Datsenko, N. M., and Karlén, W.:  
499 Highly variable Northern Hemisphere temperatures reconstructed from low-  
500 and high-resolution proxy data, *Nature*, 433, 613-617,  
501 <https://doi.org/10.1038/nature03265>, 2005.
- 502 Oppenheimer, C., Wacker, L., Xu, J., Galván, J. D., Stoffel, M., Guillet, S., Corona, C.,  
503 Sigl, M., Di Cosmo, N., Hajdas, I., Pan, B., Breuker, R., Schneider, L., Esper,  
504 J., Fei, J., Hammond, J. O. S., and Büntgen, U.: Multi-proxy dating the  
505 ‘Millennium Eruption’ of Changbaishan to late 946 CE, *Quat. Sci. Rev.*, 158,  
506 164-171, <https://doi.org/10.1016/j.quascirev.2016.12.024>, 2017.
- 507 PAGES 2k Consortium: Continental-scale temperature variability during the past two  
508 millennia, *Nat. Geosci.*, 6, 339, <https://doi.org/10.1038/ngeo1797>, 2013.



- 509 Schneider, L., Smerdon, J. E., Büntgen, U., Wilson, R. J. S., Myglan, V. S., Kirilyanov,  
510 A. V., and Esper, J.: Revising midlatitude summer temperatures back to  
511 A.D. 600 based on a wood density network, *Geophys. Res. Lett.*, 42,  
512 4556-4562, <https://doi.org/10.1002/2015GL063956>, 2015.
- 513 Schweingruber, F. H.: *Tree rings and environment: dendroecology*, Paul Haupt AG  
514 Bern, Berne, 609 pp, 1996.
- 515 Shao, X. M. and Wu, X. D.: Reconstruction of climate change on Changbai Mountain,  
516 northeast China using tree-ring data, *Quaternary Science*, 1, 76-85 (in Chinese  
517 with English abstract), 1997.
- 518 Stone, L., Saparin, P. I., Huppert, A., and Price, C.: El Niño Chaos: The role of noise  
519 and stochastic resonance on the ENSO cycle, *Geophys. Res. Lett.*, 25, 175-178,  
520 <https://doi.org/10.1029/97GL53639>, 1998.
- 521 Sun, C., You, H., Liu, J., Li, X., Gao, J., and Chen, S.: Distribution, geochemistry and  
522 age of the Millennium eruptives of Changbaishan volcano, Northeast China —  
523 A review, *Frontiers of Earth Sci.*, 8, 216-230,  
524 <https://doi.org/10.1007/s11707-014-0419-x>, 2014.
- 525 Torrence, C. and Compo, G. P.: A Practical Guide to Wavelet Analysis, *Bull. Am.*  
526 *Meteorol. Soc.*, 79, 61-78,  
527 [https://doi.org/10.1175/1520-0477\(1998\)079<0061:APGTWA>2.0.CO;2](https://doi.org/10.1175/1520-0477(1998)079<0061:APGTWA>2.0.CO;2),  
528 1998.
- 529 Wang, J., Yang, B., Osborn, T. J., Ljungqvist, F. C., Zhang, H., and Luterbacher, J.:



- 530 Causes of East Asian Temperature Multidecadal Variability Since 850 CE,  
531 Geophys. Res. Lett., 45, 13,485-13,494,  
532 <https://doi.org/10.1029/2018GL080725>, 2018.
- 533 Wang, X., Zhang, M., Ji, Y., Li, Z., Li, M., and Zhang, Y.: Temperature signals in  
534 tree-ring width and divergent growth of Korean pine response to recent  
535 climate warming in northeast Asia, *Trees*, 31, 415-427,  
536 <https://doi.org/10.1007/s00468-015-1341-x>, 2017.
- 537 Wei, H., Sparks, R. S. J., Liu, R., Fan, Q., Wang, Y., Hong, H., Zhang, H., Chen, H.,  
538 Jiang, C., Dong, J., Zheng, Y., and Pan, Y.: Three active volcanoes in China  
539 and their hazards, *J. Asian Earth Sci.*, 21, 515-526,  
540 [https://doi.org/10.1016/S1367-9120\(02\)00081-0](https://doi.org/10.1016/S1367-9120(02)00081-0), 2003.
- 541 Wigley, T. M. L., Briffa, K. R., and Jones, P. D.: On the Average Value of Correlated  
542 Time Series, with Applications in Dendroclimatology and Hydrometeorology,  
543 *J. Clim. Appl. Meteorol.*, 23, 201-213,  
544 [https://doi.org/10.1175/1520-0450\(1984\)023<0201:OTAVOC>2.0.CO;2](https://doi.org/10.1175/1520-0450(1984)023<0201:OTAVOC>2.0.CO;2),  
545 1984.
- 546 Xu, J., Pan, B., Liu, T., Hajdas, I., Zhao, B., Yu, H., Liu, R., and Zhao, P.: Climatic  
547 impact of the Millennium eruption of Changbaishan volcano in China: New  
548 insights from high-precision radiocarbon wiggle-match dating, *Geophys. Res.*  
549 *Lett.*, 40, 54-59, <https://doi.org/10.1029/2012GL054246>, 2013.
- 550 Yang, B., Braeuning, A., Johnson, K. R., and Shi, Y.: General characteristics of



- 551 temperature variation in China during the last two millennia, *Geophys. Res.*  
552 *Let.*, 29, L014485, <https://doi.org/10.1029/2001GL014485>, 2002.
- 553 Yin, J., Jull, A. J. T., Burr, G. S., and Zheng, Y.: A wiggle-match age for the  
554 Millennium eruption of Tianchi Volcano at Changbaishan, Northeastern China,  
555 *Quat. Sci. Rev.*, 47, 150-159, <https://doi.org/10.1016/j.quascirev.2012.05.015>,  
556 2012.
- 557 Yonenobu, H. and Eckstein, D.: Reconstruction of early spring temperature for central  
558 Japan from the tree-ring widths of Hinoki cypress and its verification by other  
559 proxy records, *Geophys. Res. Lett.*, 33, L10701,  
560 <https://doi.org/10.1029/2006GL026170>, 2006.
- 561 Yu, S., Yuan, Y., Wei, W., Chen, F., Zhang, T., Shang, H., Zhang, R., and Qing, L.: A  
562 352-year record of summer temperature reconstruction in the western  
563 Tianshan Mountains, China, as deduced from tree-ring density, *Quat. Res.*, 80,  
564 158-166, <https://doi.org/10.1016/j.yqres.2013.05.005>, 2013.
- 565 Yuan, Y. and Yang, S.: Impacts of Different Types of El Niño on the East Asian  
566 Climate: Focus on ENSO Cycles, *J. Clim.*, 25, 7702-7722,  
567 <https://doi.org/10.1175/JCLI-D-11-00576.1>, 2012.
- 568 Yun, S.-H.: Volcanological Interpretation of Historical Eruptions of Mt. Baekdusan  
569 Volcano, *J. Korean Earth Sci. Soc.*, 34, 456-469, 2013.
- 570 Zhang, T., Yuan, Y., Liu, Y., Wei, W., Zhang, R., Chen, F., Yu, S., Shang, H., and Qin,  
571 L.: A tree-ring based temperature reconstruction for the Kaiduhe River



572 watershed, northwestern China, since A.D. 1680: Linkages to the  
573 North Atlantic Oscillation, *Quat. Int.*, 311, 71-80,  
574 <https://doi.org/10.1016/j.quaint.2013.07.026>, 2013.

575 Zhou, Y., Liu, L., Zhang, M., and Yu, J.: Medicinal plant resources and their diversity  
576 in Changbai Mountain National Nature Reserve, *Scientia Silvae Sinicae*, 41,  
577 57-64, 2005.

578 Zhu, H. F., Fang, X. Q., Shao, X. M., and Yin, Z. Y.: Tree ring-based February–April  
579 temperature reconstruction for Changbai Mountain in Northeast China and its  
580 implication for East Asian winter monsoon, *Clim. Past*, 5, 661-666,  
581 <https://doi.org/10.5194/cp-5-661-2009>, 2009.

582 Zhu, Y., Chen, L., and Yu, R.: Analysis of the relationship between the China  
583 anomalous climate variation and ENSO cycle on the quasi-four-year scale, *J.*  
584 *Trop. Meteorol.*, 19, 345-356,  
585 <https://doi.org/10.3969/j.issn.1006-8775.2004.01.001>, 2004.